Molecular Vision 2016; 22:827-835 <http://www.molvis.org/molvis/v22/827>
Received 30 December 2015 | Accepted 16 July 2016 | Published 19 July 2016

Genetic analysis of Tunisian families with Usher syndrome type 1: toward improving early molecular diagnosis

Imen Ben-Rebeh,[1] Mhamed Grati,[2] Crystel Bonnet,[3] Walid Bouassida,[4] Imen Hadjamor,[1] Hammadi Ayadi,[1] Abdelmonem Ghorbel,[5] Christine Petit,[2,3,6] Saber Masmoudi[1]

[1]Laboratoire de Procédés de criblage moléculaire et cellulaire, Centre de Biotechnologie de Sfax, Université de Sfax, Tunisie; [2]Unité de Génétique et Physiologie de l'Audition, INSERM UMRS 1120, Institut Pasteur, Paris, France; [3]INSERM UMRS 1120, Institut de la Vision, Paris, France; [4]Service d'Ophtalmologie, C.H.U. H. Bourguiba de Sfax, Tunisie; [5]Service d'O.R.L., C.H.U.H. Bourguiba de Sfax, Tunisie; [6]Collège de France, Paris, France

Purpose: Usher syndrome accounts for about 50% of all hereditary deaf-blindness cases. The most severe form of this syndrome, Usher syndrome type I (USH1), is characterized by profound congenital sensorineural deafness, vestibular dysfunction, and retinitis pigmentosa. Six USH1 genes have been identified, *MYO7A*, *CDH23*, *PCDH15*, *USH1C*, *SANS,* and *CIB2*, encoding myosin VIIA, cadherin-23, protocadherin-15, harmonin, scaffold protein containing ankyrin repeats and a sterile alpha motif (SAM) domain, and calcium- and integrin-binding member 2, respectively.
Methods: In the present study, we recruited four Tunisian families with a diagnosis of USH1, together with healthy unrelated controls. Affected members underwent detailed audiologic and ocular examinations. We used the North African Deafness (NADf) chip to search for known North African mutations associated with USH. Then, we selected microsatellite markers covering USH1 known loci to genotype the DNA samples. Finally, we performed DNA sequencing of three known USH1 genes: *MYO7A*, *PCDH15*, and *USH1C*.
Results: Four biallelic mutations, all single base changes, were found in the *MYO7A*, *USH1C*, and *PCDH15* genes. These mutations consist of a previously reported splicing defect c.470+1G>A in *MYO7A*, three novel variants, including two nonsense (p.Arg3X and p.Arg134X) in *USH1C* and *PCDH15*, respectively, and one frameshift (p.Lys615Asnfs*6) in *MYO7A*.
Conclusions: We found a remarkable genetic heterogeneity in the studied families with USH1 with a variety of mutations, among which three were novel. These novel mutations will be included in the NADf mutation screening chip that will allow a higher diagnosis efficiency of this extremely genetically heterogeneous disease. Ultimately, efficient molecular diagnosis of USH in a patient's early childhood is of utmost importance, allowing better educational and therapeutic management.

Usher syndrome (USH) is an autosomal recessive disease in which sensorineural hearing impairment (HI) is associated with retinitis pigmentosa (RP) causing progressive retina photoreceptor degeneration [1,2]. Moreover, some patients suffer from vestibular dysfunction. USH is usually distinguished in three subtypes [3]. Individuals with Usher syndrome type 1 (USH1), the most severe form, are generally born completely deaf or lose most of their hearing early. Deafness is then followed by progressive visual impairment caused by RP, which usually becomes apparent in childhood. Patients often have difficulties maintaining their balance owing to problems in their vestibular system. USH1 (OMIM 276900) is genetically heterogeneous, and thus far, six USH1 genes have been identified: *MYO7A* (Gene ID:4647; OMIM 276903), *USH1C* (Gene ID:10083; OMIM 605242), *CDH23* (Gene ID: 64072; OMIM 605516), *PCDH15* (Gene ID:65217; OMIM 605516), *USH1G* (Gene ID: 124590; OMIM 607696), and *CIB2* (Gene ID:10518; OMIM 605564) [4]. The range of prevalence of USH1 is 3.2–6.2/100,000 depending on the study [5]. Variants in the *MYO7A* gene cause the most common form of USH1, USH1B, accounting for approximately 50% of cases; approximately 30% of cases associated are with mutations in *CDH23* and *PCDH15* [6]. Mutations in *MYO7A* [7,8], *USH1C* [9], *CDH23* [10], *PCDH15* [11], and *CIB2* [12] have also been reported in patients affected by non-syndromic HI. Remarkably, the identified USH genes encode for proteins from different classes and families with different functions. *MYO7A* encodes actin-based molecular motor known to transport cargos and position sensory hair cell stereocilia upper tip-link insertion (UTLI) complex thus tensing the tip-link. *USH1C* encodes multipostsynaptic density, disc large, zonula occludens (PDZ) domain-containing protein harmonin [13], known as the central organizer of the sub-membranous UTLI

Correspondence to: Imen Ben Rebeh, Laboratoire de Procédés de criblage moléculaire et cellulaire, Centre de Biotechnologie de Sfax, Route de Sidi Mansour Km6, BP"1177," 3018, Sfax, Tunisie; Phone: 0021674871816; FAX: 0021674875818; email: benrebah@gmail.com.
Dr. Grati is now at Department of Otolaryngology, University of Miami Miller School of Medicine, Miami, FL, 33136.

complex. Mutations in the genes encoding two cadherin-related proteins, cadherin 23 and protocadherin 15 that form the integral plasma membrane stereocilia tip-links, underlie USH1D [14] and USH1F [15], respectively. *SANS* (Gene ID: 124590) encodes an UTLI scaffold protein containing ankyrin repeats and a sterile alpha motif (SAM) domain. Finally, alterations of the calcium- and integrin-binding member 2 cause USH1J. Growing evidence suggests that these proteins are organized in a protein "interactome" in the inner ear and the retina, which is critical for the development, maintenance, and correct function of the sensorineural cells.

Genetic analysis of patients with USH is complicated by the large number of genes involved in USH and the many exons comprising the coding regions of these genes. Therefore, patients with USH are studied genetically by linkage analysis in those informative families, or gene by gene, according to their established prevalence in the analyzed population. This method is costly and a burden on medical resources, as well as being time-consuming. Microarray approaches have been used for screening for specific mutations in HI genes and have demonstrated accurate and reliable results [16]. A specific genotyping microarray for USH was developed by Asper Biotech (Tartu, Estonia) to facilitate the genetic study of patients. Cremers et al. [17] evaluated the first version of the microarray, detecting mutations in 46% of patients with USH1, 24% of patients with USH2, 29% of patients with USH3, and 30% of patients with atypical USH. Chakchouk et al. [16] designed a cost-effective North African Deafness (NADf) chip for rapid and simultaneous analysis of 58 mutations using multiplex PCR coupled with a dual-color arrayed primer extension. Recent technological advances in target-enrichment methods and next-generation sequencing offer a unique opportunity to break through the barriers of limitations imposed by gene arrays [18]. However, implementing such technology for clinical diagnosis is expensive in developing countries. In addition, managing, analyzing, and interpreting data easily and clearly for clinical purposes such as the NADf chip is not feasible.

In the present study, we report the results of a genetic investigation of four Tunisian families with USH1. First, we used the NADf chip, an APEX-based microarray for genotyping assays of USH-associated genes in Tunisia only for known and confirmed mutations. We identified only one splice-site variant in the *MYO7A* gene that has been previously described. For the other genes, a total of three novel variants, two nonsense and one frameshift mutation, were detected with sequencing analysis.

METHODS

Family and clinical data: Four Tunisian consanguineous families from southern Tunisia (the Sfax and Douz regions) with a clinical diagnosis of USH1 (28 patients) and control subjects were sampled and studied. In the Table 1 we provide all information about patient gender and age. The ethics committee of the University Hospital of Sfax (Tunisia) approved this study. Written informed consents were obtained from both parents. Our study adhered to the tenets of the Declaration of Helsinki and The Association for Research in Vision and Ophthalmology (ARVO) statement on human subjects. The pedigrees were drawn after interviews with the parents (Figure 1).

Twenty-eight members from the four Tunisian families (11 male and 17 female members) were subjected to audiologic examination. The degree of HI was assessed with the pure audiometry test for air and bone conduction at the 0.25, 0.5, 1, 2, 4, and 8 kHz frequencies for each ear. Vestibular function was evaluated based on the caloric test. For ophthalmology examinations, dilated funduscopy was performed for all patients. Electroretinography (ERG) and an automated visual field test were performed only on two patients with sine pigmento fundus appearance to improve the visualization of the retinal dystrophy (USHTF1IV5, USHTF4II3). Patients were identified as having USH1 according to the criteria recommended by the Usher Syndrome Consortium [19]. Clinical history and physical examinations of family members ruled out the implication of environmental factors in the etiology of HI and RP. Blood samples were collected, and genomic DNA was extracted using standard methods. Blood samples were collected in EDTA tubes, mixed by inversion 8-10 times after being drawn and stored at 4 °C for up to a month prior to gDNA isolation. Phenol–chloroform extraction technique was used to purify nucleic acids and to eliminate proteins and lipids. In brief, aqueous samples are mixed with equal volumes of a phenol:chloroform mixture. After mixing, the mixture is centrifuged and two distinct phases are formed. The proteins and hydrophobic lipids will partition into the lower organic phase while the nucleic acids remain in the upper aqueous phase.

Microsatellite genotyping: To determine whether USH1 syndrome in these families is linked to one of the known loci, microsatellite markers were selected based on their map position and heterozygosity coefficient (UCSC Genome Browser). Microsatellite markers were genotyped for all participating family members (Table 2). Fluorescently-labeled alleles were analyzed on an ABI Prism 3100-Avant automated DNA Analyzer (Applied Biosystems, Foster City, CA).

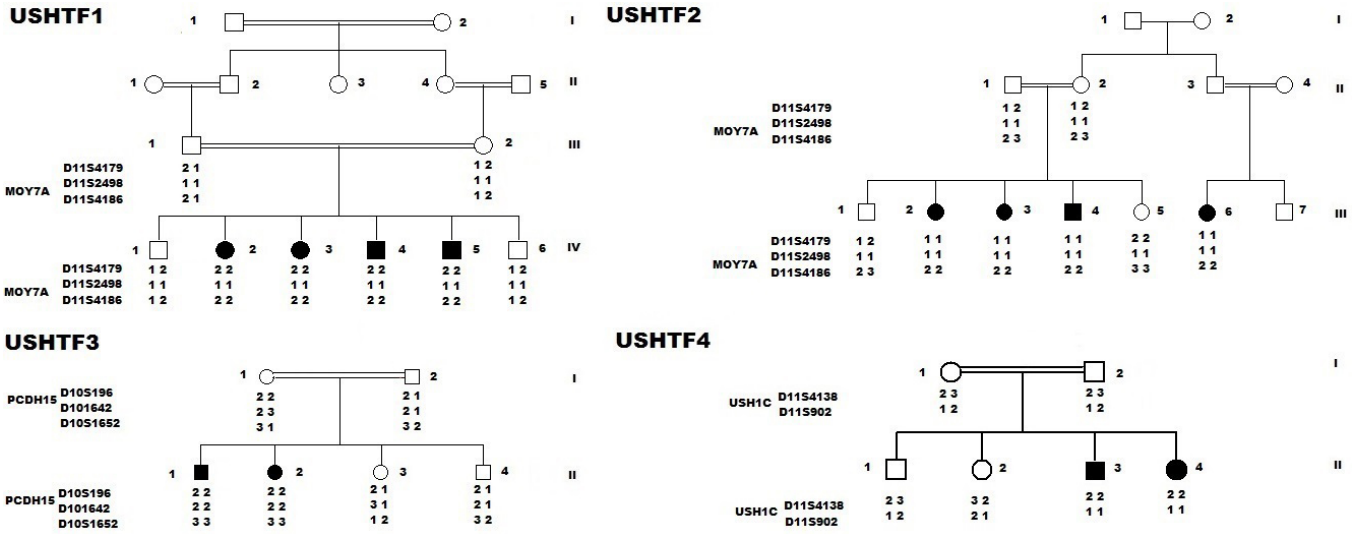

Figure 1. Pedigree and haplotype for four consanguineous Tunisian families who segregate Usher type 1. In the pedigree, the square symbol indicates male, the circle symbol denotes female, and the black squares represent affected individuals. Linkage analysis performed on all families showed that two were linked to USH1B, and the remaining families with USH1 were linked to USH1C and USH1F.

Mutation screening: Screening of known North African mutations associated with USH was performed with a cost-effective NADf chip using multiplex-PCR coupled with dual-color arrayed primer extension as described by Chakchouk et al. [16]. Multiplex-PCR was performed in a total volume of 50 µl, including 40 µl of the 12 multiplex PCR fragmented products, 0.5 µl of each fluorescent ddNTP, and 1 U of thermosequenase (GE Healthcare, Chalfont St. Giles, UK). Arrays were hybridized with the reaction mixture for 30 min at 60 °C using the FAST Frame Cassette (Sigma-Aldrich, Dorset, UK). The arrays were then washed briefly with 0.3% Alconox detergent (Sigma-Aldrich, Munich, Germany) and distilled water. Slides were then dried before scanning. The coding exons and flanking intronic sequences of all three USH1 genes (*MYO7A*, *USH1C*, and *PCDH15)* were amplified using forward and reverse primers. Mutations were identified by sequencing the PCR products from one affected individual from each family on an ABI Prism 3100-Avant automated

Table 1. Clinical information of patients with pathogenic mutations.

Families	Age	Sex	Age of clinic examination	Fundus of the eye	Visual field	ERG	Caloric test	Severity of HI
USHTF1IV2	22	F	12	RP	ND	ND	BP	Profound
USHTF1IV3	25	F	15	RP	ND	ND	BP	Profound
USHTF1IV4	33	M	23	RP	ND	ND	BP	Profound
USHTF1IV5	**40**	M	**30**	RP	5–10° (V/4e)	Done	BP	Profound
USHTF2III2	29	F	19	RP	ND	ND	BP	Profound
USHTF2III3	27	F	17	RP	ND	ND	BP	Profound
USHTF2III4	**35**	M	25	RP	ND	ND	BP	Profound
USHTF2III6	25	F	15	RP	ND	ND	BP	Profound
USHTF3II1	22	M	12	RP	ND	ND	BP	Profound
USHTF3II2	13	F	3	RP	ND	ND	BP	Profound
USHTF4II3	**47**	F	**37**	RP	5–10° (V/4e)	Done	BP	Profound
USHTF4II4	33	M	23	RP	ND	ND	BP	Profound

Abbreviations: ERG: electroretinography; HI: hearing impairment; RP: Retinitis pigmentosa; BP: Balance Problems. ND: Not done.

DNA Analyzer (Applied Biosystems). Exons harboring mutations were amplified on 40 ng genomic DNA, and then either Sanger sequencing or PCR-restriction fragment length polymorphism (RFLP) analysis was used to examine whether the mutations segregated with the disease in the families and were not present in the 50 control individuals.

RESULTS

The pedigrees in Figure 1 display four consanguineous Tunisian families originating from two regions of Tunisia and segregating USH1, based on clinical, audiometric, and ophthalmologic data. The audiometric test showed profound congenital and bilateral sensorineural hearing loss. Vestibular dysfunction was detected in all patients using the caloric test (Table 1). Parents reported that their children presented a delay in motor development and began sitting independently and walking later than usual.

Onset of retinitis pigmentosa occurs during childhood, resulting in a progressively constricted visual field and night blindness. The fundus examination detected retinal degeneration in all of the patients (Table 1). The visual fields (Goldmann targets III/4e) of two older patients were significantly reduced to a 5° concentric field and temporal island fields for both eyes (Figure 2). The Ganzfeld-ERG recorded in the same patients showed an almost normal response flash visual-evoked potential in both eyes and significant bilateral global retinal degeneration. Only cone flicker responses of less than 15% of the normal mean were recordable under photopic conditions while all other responses were below noise level, a typical finding for patients with RP (Figure 2). Taken together, the clinical signs observed in the affected subjects indicated a form of USH1.

First, known North African mutations associated with USH were analyzed with a cost-effective NADf chip using multiplex PCR coupled with a dual-color arrayed primer extension [16]. In one family, one previously reported splicing defect-causing mutation was detected. The known variant was a nucleotide substitution (c.470+1G>A) [8] that is predicted to alter the splice donor site of intron 5 and to result in the skipping of exon 5 in the mature transcript. This DNA variant was analyzed with the following programs: NNSPLICE, which evaluates the strength of splice sites [20], and Human Splicing Finder (HSF) [21],which includes several matrices for analyzing splice sites and splicing silencers and enhancers (for example, MaxEnt, ESEfinder, and PESX). Second, linkage analysis performed on all three remaining USH1 families showed that one member of each family was linked to USH1B, USH1C, and *USH1F* loci. Finally, the direct sequencing of *MYO7A*, *USH1C*, and *PCDH15* detected a total of three distinct novel pathogenic mutations: one frameshift mutation, and two nonsense mutations (Figure 3). The frameshift mutation is caused by nucleotide deletion c.1845delG that leads to a premature stop codon at position 615 (p.Lys615Asnfs*6) with probably a loss of 72% of the C-terminal region of the protein. The remaining two nonsense mutations p.Arg3X and p.Arg134X were revealed in *USH1C* and *PCDH15*, respectively. According to Alamut 2.3 Interactive Biosoftware (Rouen, France), these truncating mutations are expected to result in the absence of synthesized protein due to mRNA nonsense mediated decay. All of the mutations reported here were observed in a homozygous state. In addition, all new variants were not present in the exome variant server (EVS) database (6448 exomes) and dbSNP databases and were absent from the Tunisian control samples (Table 3).

Table 2. Fluorescent dye-labeled microsatellite markers were genotyped for linkage analysis in four USH1 Tunisian consanguineous families.

Markers	Position (UCSC genome browser)
***MYO7A* gene**	
D11S4179	Chr11:76685129–76685482
D11S2498	Chr11:76.336.884–76337044
D11S4186	Chr11: 77,257,402-77257673
***PCDH15* gene**	
D10S196	Chr10 :50382508–50382689
D10S1642	Chr10 :54655145–54655555
D10S1652	Chr10 :62647735–62648093
USH1C gene	
D11S4138	Chr 11:17734173–17734429
D11S902	Chr11 :17466895–17467129

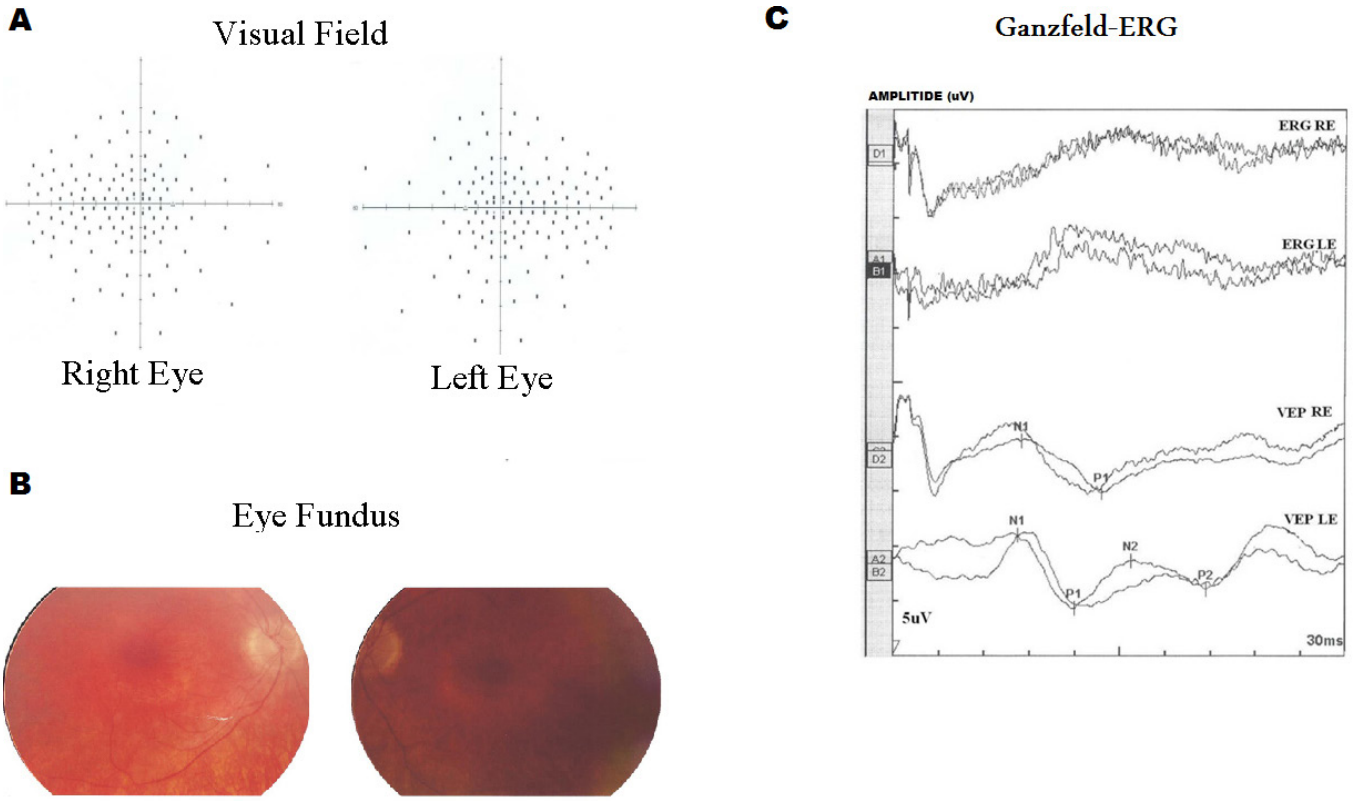

Figure 2. Visual field test results obtained for the right (RE) and the left eye (LE) of two patients (USHTF1IV5, USHTF4II3). **A**: Result of measurements of the visual fields. **B**: Result of eye fundus measurement. A series of random lights of different intensities were flashed in the peripheral field of vision of both patients. When they perceived the computer-generated light that suddenly appeared in their field of view, they pressed a button to indicate their responses, and then we saw this spot (Dot see). If the patient was unable to see the light in an appropriate portion of his field of view, then we saw on the computer a spot (Dot don't see) indicating vision loss. In all patients, the nasal and temporal fields were not preserved, and only the central field was maintained. Fundus ophthalmoscopy showed pigmentary anomalies typical of retinitis pigmentosa (RP), attenuated arteriolar vessels and increased brightness of the internal limiting membrane. The visual field showed an anular scotoma reduced by 15°. **C**: Ganzfeld-Electroretinogram of the right and left eyes of two patients (USHTF1IV5, USHTF4II3). The electroretinogram (ERG) and the visual-evoked potential (VEP) test the function of the visual pathway from the retina (ERG) to the occipital cortex (VEP). These tests were conducted by placing a standard ERG device attached to the skin on 2 mm above the orbit. VEPs were recorded simultaneously from the electrode attached to the occipital scalp 2 mm above the region on the midsagittal plane. An electrode placed on the forehead provided a ground. The results are directly related to the part of a visual field that might be defective. This is based on the anatomic relationship of the retinal images and the visual field. After dark adaptation for 30 min, the doctor placed anesthetic drops in the patient's eye and placed a contact lens on the surface of the eye. Once the contact lens was in place, a series of blue, red, and white lights were shown to the patient. The VEP is an evoked electrophysiological potential that can be extracted, using signal averaging, from the electroencephalographic activity recorded at the scalp. ERG and VEP were differentially amplified band pass filtered (0,1,30 Hz), recorded over 300 ms epochs, and the signals averaged. Two trials were given. The visual evoked potential to flash stimulation consists of a series of negative and positive waves. The earliest detectable response has a peak latency of approximately 30 ms post-stimulus. For the flash VEP, the most robust components are the N2 (negative) and P2 (positive) peaks. Measurements of the P2 amplitude should be made from the positive P2 peak at around 207.3 ms. The ERG recorded in BT189 showed an absence of responses although the VEP showed a normal responses in both eyes. These traces confirm evidence of significant bilateral global retinal degeneration. Only cone flicker responses of less than 15% of the normal mean were recordable under photopic conditions while all other responses were below noise level, a typical finding for patients with retinitis pigmentosa.

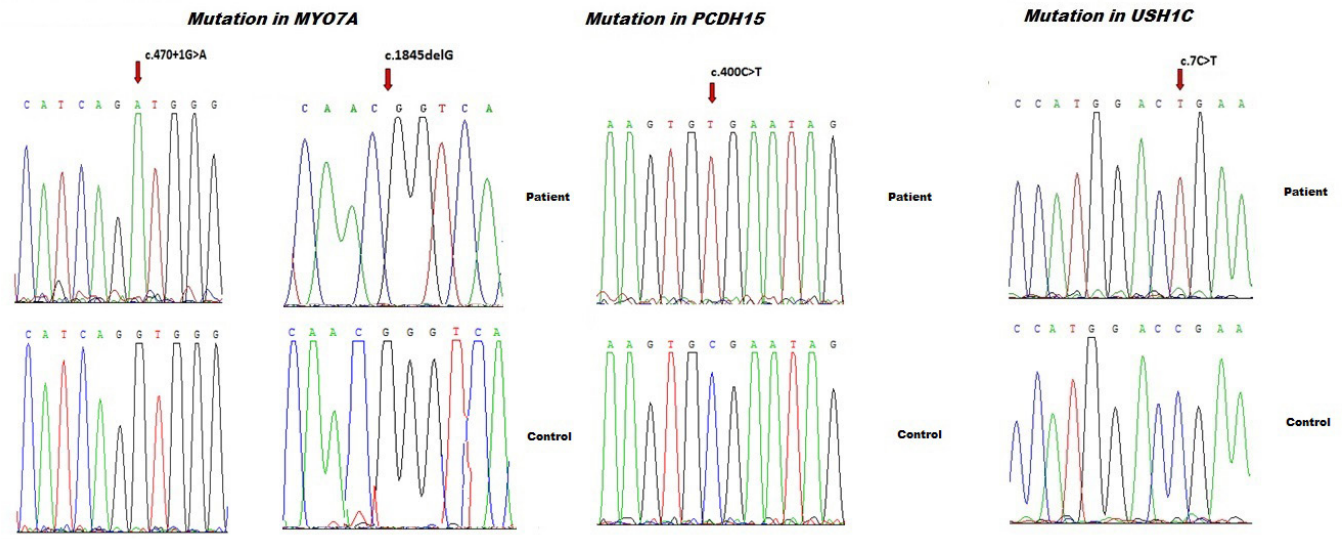

Figure 3. The direct sequencing of *MYO7A*, *USH1C*, and *PCDH15* detected a total of three distinct novel pathogenic mutations: one frameshift mutation, two nonsense mutations, and one previously reported splicing defect-causing mutation. The known variant was a nucleotide substitution (c.470+1G>A), and the frameshift mutation is caused by nucleotide deletion c.1845delG causing USH1B. The molecular screening of *USH1C* and *PCDH15* revealed two novel nonsense mutations occurring at the homozygous state: p.Arg3X in *USH1C* and p.Arg134X in *PCDH15*.

DISCUSSION

Here, we report the results of genomic DNA linkage and mutation analyses of four Tunisian families with USH1 according to the audiologic and ophthalmologic evaluations. The examinations showed that the vestibular reflexes were abnormal in the patients, and the audiometric and ocular findings did not differ from what has been previously reported [19]. Molecular studies confirmed our clinical classification of the four families as USH1 with mutations in *MYO7A*, *USH1C*, and *PCDH15* genes. It is well documented that mutations in these genes can cause USH1 and nonsyndromic HI, DFNB2, DFNB18, and DFNB23, respectively [9,11,22]. Moreover, clinically atypical cases that do not fit the three definitions of USH have also been reported with mutations in these genes. However, the clinical findings did not suggest any obvious clinical variance between families.

Table 3. Frequency of USH1 genes in Tunisian population.

Tunisian Famillies	Linkage	Gene	Mutation	Protein change	References
USHTF1	USH1B	MYO7A	470+1G>A	-	[8]
USHTF2	USH1B	MYO7A	470+1G>A	-	Our study
USHTF3	USH1B	MYO7A	c.1935G>A	-	[22]
USHTF4	USH1B	MYO7A	c.1935G>A	-	[23]
USHTF5	USH1B	MYO7A	c.2283–1G>T	-	[21]
USHTF6	USH1B	MYO7A	c.5434G>A	p.Glu1812Lys	[21]
USHTF7	USH1B	MYO7A	c.1845delG	p.Lys615Asnfs*6	Our study
USHTF8	USH1C	USH1C	c.91C>T	-	[16]
USHTF9	USH1C	USH1C	c.7C>T	p.R3X	Our study
USHTF10	USH1F	PCDH15	c.400C>T	p.R134X	Our study
USHTF11	USH1G	SANS	c.393insG	-	[33]
USHTF12	USH1G	SANS	c.393insG	-	[16]
USHTF13	USH1G	SANS	c.1195_1196delAG	p.Leu399Alafs*24	[21]
USHTF14	USH1G	SANS	c.52A>T	-	[21]

NADf chip analysis and Sanger sequencing of *MYO7A* resulted in the identification of two pathological mutations, c.470+1G>A and p.Lys615Asnfs*6, causing USH1B. The splicing defect-causing mutation has been previously reported by Adato et al. [8] in Tunisian patients. Recently, whole exome sequencing of Tunisian families affected by typical Usher syndrome allowed the identification of an additional splice acceptor site mutation, c.2283–1G>T, and a novel missense mutation, c.5434G>A (p.Glu1812Lys) in the *MYO7A* gene [22]. Mutations in *MYO7A* have also been reported in two Tunisian families affected by atypical Usher syndrome [23,24]. These data confirm the presence of a wide range of heterogeneity in *MYO7A* in the Tunisian population. However, at least two founder mutations (c.470+1G>A and c.1935G>A) were identified [16]. This observation may reflect the relative isolation and marriage patterns among the Tunisian population.

However, the two remaining families were linked to *USH1C* and *USH1F*, respectively. The molecular screening of *USH1C* and *PCDH15* revealed two novel nonsense mutations occurring at the homozygous state: p.Arg3X in *USH1C* and p.Arg134X in *PCDH15*. Linkage and mutation analyses have indicated that 29–82% of USH1 cases are possibly the result of a mutation in MYO7A, depending on the population and number of exons screened [25,26]. For USH1, Kimberling et al. [27] evaluated the mutation frequency as about 5% in USH1C, 10% in *CDH23*, and rare for *PCDH15* and *SANS*, indicating that *MYO7A* is the major cause of USH1. In the Tunisian population, molecular studies have also confirmed that mutations in *MYO7A* are the major cause for USH1 (Table 3). *SANS* is the second most common cause, while mutations in *USH1C*, *CDH23*, *PCDH15*, and *CIB2* are less frequent in Tunisian families. In fact, seven of 14 (50%) families with USH1 were linked to the *USH1B* locus, while four families with type 1 were linked to *USH1G*, two families with type 1 were linked to the *USH1C* locus, and the remaining family was linked to the *USH1F* locus (Table 3). These data provide an initial estimate of the proportion of the various type 1 Usher syndrome subtypes in the Tunisian deaf population and support the notion of high genetic heterogeneity in that population.

Early diagnosis of USH1 is critical for genetic counseling and adapted educational and therapeutic management, which may include retinal gene therapy in the future [28,29]. Delayed walking is suggested to be the earliest clinical sign of Usher syndrome in deaf children [30]. In consanguineous families, homozygosity mapping remains a powerful method for mapping recessive traits. The method takes advantage of the fact that intermarried affected individuals are likely to have identical by descent alleles at markers located near the disease locus and thus will be homozygous at these markers [31]. However, consanguinity and endogamy in a population lead to genetic homogeneity with several homozygous genomic regions and few informative markers. In addition, after homozygosity, mapping genetic analysis of patients with USH is complicated by the large number of exons comprising the coding regions of USH genes. Recently, different high-throughput sequencing strategies were developed for the detection of mutations in USH-associated genes [32]. However, implementing such technology for clinical diagnosis is expensive in developing countries. In addition, managing, analyzing, and interpreting the data for clinical purposes present many challenges. The high number of polymorphic variations and the correct interpretation of sequence variations with no obvious pathogenic role limit the use of such strategies. The microarray assay interrogates only for known and confirmed mutations. Interestingly, the NADf chip allows the detection of 18 known mutations associated with USH1 in North African families [16]. All of the equipment and reagents required to carry out the NADf chip assay are generally available in molecular laboratories. In addition, despite the genetic heterogeneity of USH in Tunisia, at least two founder mutations were described. Hopefully, better knowledge of the molecular alterations underlying USH in this population and the inclusion of these novel mutations in the NADf chip may lead to a more efficient diagnosis and will encourage development of therapies for other USH1 genes. The success of these therapies will depend on our understanding of the disease progression and on selecting the appropriate time points for treatment.

In conclusion, this study in combination with previous reports on Tunisian patients with USH1 show that this syndrome is likely quite heterogeneous. Our data also provide an initial estimate of the frequency of various mutations that may lead to a more efficient diagnostic in the North African population.

ACKNOWLEDGMENTS

We are indebted to the all family members for their invaluable cooperation and for providing the blood samples. This study was supported by funds from the ICGEB (International Centre for Genetic Engineering and Biotechnology) and the Ministry of Higher Education and Research of Tunisia to SM.

REFERENCES

1. Keats BJ, Corey DP. The Usher syndromes. Am J Med Genet 1999; 89:158-66. [PMID: 10704190].

2. Bonnet C, El-Amraoui A. Usher syndrome (sensorineural deafness and retinitis pigmentosa): Pathogenesis, molecular diagnosis and therapeutic approaches. Curr Opin Neurol 2012; 25:42-9. [PMID: 22185901].

3. Smith RJ, Berlin CI, Hejtmancik JF, Keats BJ, Kimberling WJ, Lewis RA, Moller CG, Pelias MZ, Tranebjaerg L. Clinical diagnosis of the Usher syndromes. Usher Syndrome Consortium. Am J Med Genet 1994; 50:32-8. [PMID: 8160750].

4. Kinga MB, Mark C, Emily P, Shyana H, Jaclyn L, Daniel GT, Joseph W, Daniel NG, Carol WD, Michael HF, Xiaowu G, Eliot LB. Targeted Exon Sequencing in Usher Syndrome Type I. Biochemistry and Molecular Biology. 2014; 55:8488-96. .

5. Jose MM, Elena A, Teresa J, Fiona BK, Ascension GP, Carmen A. An Update on the Genetics of Usher Syndrome. J Ophthalmol 2011; •••:8-.

6. Astuto LM, Weston MD, Carney CA, Hoover DM, Cremers CW, Wagenaar M, Moller C, Smith RJ, Pieke-Dahl S, Greenberg J, Ramesar R, Jacobson SG, Ayuso C, Heckenlively JR, Tamayo M, Gorin MB, Reardon W, Kimberling WJ. Genetic heterogeneity of Usher syndrome: analysis of 151 families with Usher type I. Am J Hum Genet 2000; 67:1569-74. [PMID: 11060213].

7. Liu X-Z, Walsh J, Mburu P, Kendrick-Jones J, Cope MJTV, Steel KP, Brown SDM. Mutations in the myosin VIIA gene cause non-syndromic recessive deafness. Nat Genet 1997; 16:188-90. [PMID: 9171832].

8. Adato A, Weil D, Kalinski H, Pel-Or Y, Ayadi H, Petit C, Korostishevsky M, Bonne-Tamir B. Mutation profile of all 49 exons of the human myosin VIIA gene, and haplotype analysis in Usher 1B families from diverse origins. Am J Hum Genet 1997; 61:813-21. [PMID: 9382091].

9. Ahmed ZM, Smith TN, Riazuddin S, Makishima T, Ghosh M, Bokhari S, Menon PSN, Deshmukh D, Griffith AJ, Riazuddin S. Nonsyndromic recessive deafness DFNB18 and Usher syndrome type IC are allelic mutations of USHIC. Hum Genet 2002; 110:527-31. [PMID: 12107438].

10. Bork JM, Peters LM, Riazuddin S, Bernstein SL, Ahmed ZM, Ness SL, Polomeno R, Ramesh A, Schloss M, Srisailpathy CR, Wayne S, Bellman S, Desmukh D, Ahmed Z, Khan SN, Kaloustian VM, Li XC, Lalwani A, Riazuddin S, Bitner-Glindzicz M, Nance WE, Liu XZ, Wistow G, Smith RJ, Griffith AJ, Wilcox ER, Friedman TB, Morell RJ. Usher syndrome 1D and nonsyndromic autosomal recessive deafness DFNB12 are caused by allelic mutations of the novel cadherinlike gene CDH23. Am J Hum Genet 2001; 68:26-37. [PMID: 11090341].

11. Ahmed ZM, Riazuddin S, Ahmad J, Bernstein SL, Guo Y, Sabar MF, Sieving P, Riazuddin S, Griffith AJ, Friedman TB, Belyantseva IA, Wilcox ER. PCDH15 is expressed in the neurosensory epithelium of the eye and ear and mutant alleles are responsible for both USH1F and DFNB23. Hum Mol Genet 2003; 12:3215-23. [PMID: 14570705].

12. Saima R, Inna AB, Arnaud PJG, Kwanghyuk L, Artur AI, Sri Pratima N, Rizwan Y, Ghanshyam PS, Sue L. David Tl, Rashmi S H, Rana A A, Saima A, Paula B A, Asli S, Leslie V P, Sulman B, Abdul W, Muhammad A, Muhammad A, Wasim A, Shaheen N K, Javed A, Mustafa T, Sheikh R. Alterations of the CIB2 calcium- and integrin-binding protein cause Usher syndrome type 1J and nonsyndromic deafness DFNB48. Nat Genet 2012; 44:1265-71. [PMID: 23023331].

13. Verpy E, Leibovivici M, Zwaenepoel I, Liu XZ, Gal A, Salem N, Mansour A, Blanchard S, Kobayashi I, Keats BJ, Slim R, Petit C. A defect in harmonin, a PDZ domain-containing protein expressed in the inner ear sensory hair cells, underlies Usher syndrome type 1C. Nat Genet 2000; 26:51-5. [PMID: 10973247].

14. Bolz H, von Brederlow B, Ramirez A, Bryda EC, Kutsche K, Nothwang HG, Seeliger M. del C-Salcedo Cabrera M, Vila MC, Molina OP, Gal A, Kubisch C. Mutation of CDH23, encoding a new member of the cadherin gene family, causes Usher syndrome type 1D. Nat Genet 2001; 27:108-12. [PMID: 11138009].

15. Ahmed ZM, Riazuddin S, Bernstein SL, Ahmed Z, Khan S, Griffith AJ, Morell RJ, Friedman TB, Riazuddin S, Wilcox ER. Mutations of the protocadherin gene PCDH15 cause Usher syndrome type 1F. Am J Hum Genet 2001; 69:25-34. [PMID: 11398101].

16. Imen C, Mariem BS, Fida J, Riadh BM, Salma L, Ibtihel S, Amine C, Abdullah AG, Abdelmonem G, Hassen H, Saber M. NADf Chip, a Two-Color Microarray for Simultaneous Screening of Multigene Mutations Associated with Hearing Impairment in North African Mediterranean Countries. J Mol Diagn 2015; 17:2-[PMID: 25528186].

17. Cremers FP, Kimberling WJ, Külm M. Development of a genotyping microarray for Usher syndrome. J Med Genet 2007; 44:153-60. [PMID: 16963483].

18. Zied R, Crystel B, Rim Z, Saida L, Yosra B, Rym B, Jihène M, Jean-Pierre H, Malek L, Leila L, Salim BY, Moncef K, Leila E, Ghazi B, Sonia A, Christine P. Whole Exome Sequencing Identifies Mutations in Usher Syndrome Genes in Profoundly Deaf Tunisian Patients. PLoS ONE 2015; 10:13-71. .

19. Smith RJ, Berlin CI, Hejtmancik JF, Keats BJ, Kimberling WJ, Lewis RA, Möller CG, Pelias MZ, Tranebjaerg L. Clinical diagnosis of the Usher syndromes. Usher Syndrome Consortium. Am J Med Genet 1994; 50:32-8. [PMID: 8160750].

20. Reese MG, Eeckman FH, Kulp D, Haussler D. Improved splice site detection in Genie. J Comput Biol 1997; 4:311-23. [PMID: 9278062].

21. Desmet FO, Hamroun D, Lalande M, Collod-Beroud G, Claustres M, Beroud C. Human Splicing Finder: an online bioinformatics tool to predict splicing signals. Nucleic Acids Res 2009; 37:67-[PMID: 19339519].

22. . Riazuddin S1. Nazli S, Ahmed ZM, Yang Y, Zulfiqar F, Shaikh RS, Zafar AU, Khan SN, Sabar F, Javid FT, Wilcox ER, Tsilou E, Boger ET, Sellers JR,Belyantseva IA, Riazuddin S, Friedman TB. Mutation spectrum of MYO7A and evaluation of a novel nonsyndromic deafness DFNB2 allele with residual function. Hum Mutat 2008; 4:502-11. .

23. Imen BR, Madeleine M, Leila A, Zeineb B, Ilhem C, Jamel F, Hammadi A, Abdelmonem G, Faouzi B, Saber M. Reinforcement of a minor alternative splicing event in MYO7A due to a missense mutation results in a mild form of retinopathy, deafness and vestibular areflexia. Mol Vis 2008; 14:1719-26. [PMID: 18806881].

24. Dominique W, Polonca K, Stéphane B, Gallia L, Fabienne L-A, Mohamed D, Hammadi A, Christine P. The autosomal recessive isolated deafness, DFNB2, and the Usher 1B syndrome are allelic defects of the myosin-VIIA gene. Nat Genet 1997; 16:191-3. [PMID: 9171833].

25. Larget-Piet D, Gerber S, Bonneau D, Rozet JM, Marc S, Ghazi I, Dufier JL, David A, Bitoun P, Weissenbach J, Munnich A, Kaplan J. Genetic heterogeneity of Usher syndrome type 1 in French families. Genomics 1994; 21:138-43. [PMID: 8088781].

26. Bharadwaj AK, Kasztejna JP, Huq S, Berson EL, Dryja TP. Evaluation of the myosin VIIA gene and visual function in patients with Usher syndrome type I. Exp Eye Res 2000; 12:173-81. [PMID: 10930322].

27. Kimberling WJ, Moller C. Clinical and molecular genetics of Usher syndrome. J Am Acad Audiol 1995; 6:63-72. [PMID: 7696679].

28. Jacobson SG, Aleman TS, Cideciyan AV, Sumaroka A, Schwartz SB, Windsor EA, Traboulsi EI, Heon E, Pittler SJ, Milam AH. Identifying photoreceptors in blind eyes caused by RPE65 mutations:Prerequisite for human gene therapy success. Proc Natl Acad Sci USA 2005; 102:61776-61182. [PMID: 15837919].

29. Cideciyan AV, Hauswirth WW, Aleman TS, Kaushal S, Schwartz SB, Boye SL, Windsor EA, Conlon TJ, Sumaroka A, Roman AJ. Vision 1 year after gene therapy for Leber's congenital amaurosis. N Engl J Med 2009; 361:725-7. [PMID: 19675341].

30. Kothiyal P, Cox S, Ebert J, Husami A, Kenna MA, Greinwald JH, Aronow BJ, Rehm HL. High-throughput detection of mutations responsible for childhood hearing loss using resequencing microarrays. BMC Biotechnol 2010; 10:10-[PMID: 20146813].

31. Dominik S, Markus S, Friedhelm H. Peter Nürnberg. Homozygosity Mapper -an interactive approach to homozygosity mapping. Nucleic Acids Res 2009; 37:593-9. .

32. Danilo L, Margherita M, Ivana P, Kornelia N, Nienke W, Rossella R, Diego V, Emmanouil A. Angela D'E, Mariateresa P, Francesca D'A, Carmela Z, Francesca S, Antonella F, Hans S, Paolo G, Sandro B, Vincenzo N. Molecular Diagnosis of Usher Syndrome: Application of Two Different Next Generation Sequencing-Based Procedures. PLoS ONE 2012; 7:8-.

33. Weil D, El-Amraoui A, Masmoudi S, Mustapha M, Kikkawa Y, Lainé S, Delmaghani S, Adato A, Nadifi S, Zina ZB, Hamel C, Gal A, Ayadi H, Yonekawa H, Petit C. Usher syndrome type I G (USH1G) is caused by mutations in the gene encoding SANS, a protein that associates with the USH1C protein, harmonin. Hum Mol Genet 2003; 5:463-71. [PMID: 12588794].

Articles are provided courtesy of Emory University and the Zhongshan Ophthalmic Center, Sun Yat-sen University, P.R. China. The print version of this article was created on 19 July 2016. This reflects all typographical corrections and errata to the article through that date. Details of any changes may be found in the online version of the article.